A Computer Presentation of the Analytical and Numerical Study of Nonlinear Vibration Response for Porous Functionally Graded Cylindrical Panel

Ahmed Mouthanna[1,2(✉)], Sadeq H. Bakhy[2], and Muhannad Al-Waily[3]

[1] College of Engineering, University of Anbar, Ramadi, Anbar, Iraq
ahmed.mouthana@uoanbar.edu.iq
[2] Mechanical Engineering Department, University of Technology, Baghdad, Iraq
[3] Department of Mechanical Engineering, Faculty of Engineering, University of Kufa, Kufa, Iraq

Abstract. The current study uses a new analytical model and numerical method to present a study of free vibration carried out on a cylindrical shell panel that is simply supported and functionally graded. It is anticipated that the FG thickness attributes will be dependent on the porosity level and will change along the thickness axis in accordance with a distribution that follows a power-law. This work makes a contribution by analyzing the performance of porous FGMs, which are employed in a particularly wide variety of biomedical applications. For the purpose of determining the free vibration characteristics as well as the nonlinear vibration response, the governing equations are constructed on a first-order shear deformation theory by utilizing the Galerkin technique with the fourth-order Runge Kutta a close encounter with an incomplete FGM cylindrical shell panel and include different parameters. Parameters included are the power-law index, graded distributions of porosity, and FG thickness. With the help of both the ANSYS 2021-R1 software, a numerical investigation was carried out making use of the finite element approach, and a modal investigation was carried out. This was done in order to verify the analytical strategy.

Keywords: Porous · Materials with a Functional Grading · Theory of First-Order Shear Deformation · Analytical Investigation · Nonlinear Dynamic Response · Frequency

1 Introduction

In mechanical and construction engineering, investigating and developing new materials and structures is essential. Because of their lightweight nature and excellent mechanical properties, structures composed of advanced materials are often employed in numerous industries, including civil, mechanical, and aerospace engineering. The application in practice is normally in the shape as nanocomposite structures, Functionally Graded

A. Ortis et al. (Eds.): ICAETA 2023, CCIS 1983, pp. 57–72, 2024.
https://doi.org/10.1007/978-3-031-50920-9_5

Materials (FGM) structures, laminated, and sandwich structures [1]. In recent years, analyzing a new structure has become a popular study area for numerous material and engineering scientists. Many articles have been published about composite materials. Ranging from micro-scale (nanocomposite and FGM) to macro-scale (laminated and sandwich structures), the studies have been conducted using a variety of techniques, scales, and forms [2, 3]. In the dynamics case, numerous investigations have been done on the vibration analysis of structures [4–6]. Bagheri et al. [7] studied the geometrically nonlinear dynamic response of joined conical shells constructed of functionally graded material (FGM) subjected to thermal shock. Zhu et al. [8] employed Reddy's theory of Shear Deformation at Higher Orders with the geometric nonlinearity hypothesis (von Kármán) to investigate the relationship between nonlinear forced vibration properties and nonlinear free vibration properties of viscoelastic plates. Li and Liu [9] examined the thermal free vibration as well as buckling attitude of viscoelastic sandwich of FGM shallow shell having a core constructed of tunable auxetic honeycomb. Singh et al. [10] coupled piezoelectric sensors with time-dependent tri analytical solutions in order to investigate the free vibration of viscoelastic of orthotropic rectangular plates in-plane FG. Sahu et al. [11] presented the free vibration and damping investigation of the sandwich doubly-curved shallow shell with a viscoelastic-FGM layer as suggested by the theory of shear deformation of the first order. Moreover, there has been a significant increase in the number of investigations for shell structures constructed of FGM materials [26]. These published studies investigated the buckling properties as well as the linear and nonlinear vibration behavior in classical shell theory [12, 13]. Throughout the development of the material industry, FGM porous cores employed for lightweight structures are becoming a significant element in civil, mechanical, and aerospace engineering due to their electrical, mechanical, and thermal properties. In particular, the FG porous material has a high strength as well as an excellent energy absorption capability. Ghobadi et al. [14] investigated the influence of the various distributions of porosity on the static and dynamic behavior of sandwich FGM nanostructures under thermo-electro-elastic coupling. Esayas and Kattimani [15] studied the influence of porosity on the dynamic damping of geometrically nonlinear vibrations of an FG magneto-electro-elastic plate. Javid et al. [16] researched the free vibrational characteristics of porous FG micro-cylindrical shells with viscoelastic medium and two skins made of nanocomposite based on Biot's assumptions. According to third-order shear deformation theory, Keleshteri and Jelovica [17] sandwich panels with FG metal cores of foam were studied to determine their buckling and free vibrational behavior. Kumar H S et al. [18] approaching together transient responses and FG nonlinear free vibration of skew plate under the influence of porosity distribution. Srikarun et al. [19] researched the linear and nonlinear stability of sandwich beams with porous FG cores subjected to various types of distributed loads. Chan et al. [20] Using theory of first-order shear deformation shell, researchers were investigated free vibration with a nonlinear response of the dynamic properties of a porous functionally graded trimmed shell have aconical shap equipped with actuators of piezoelectric in warm settings. Dastjerdi and Behdinan [21] studied the free vibration characteristics of smart sandwich plates with carbon nanotube-reinforced and piezoelectric layers by employing Reddy's theory of third-order shear deformation. Yadav et al. [22] investigated statics of nonlinear of sandwich circular-cylindrical shells

consisting of two carbon nanotube-reinforced face sheets and a porous FG core by utilizing higher-order shear deformation and thickness theory. Binh et al. [23] examined the nonlinear dynamic characteristics of a porous FG toroidal shell of variable thickness subjected to thermal loads and enclosed by a medium that has elasticity. Furthermore, numerous investigations displayed the advent of the porous core in strengthening structures [24, 25]. Based on 3D elasticity, the dynamic analyses and natural frequencies of porous FG cylindrical panels and annular sector plates were determined by Babaei et al. [26]. Li et al. [27] used the differential quadrature method to study the natural vibration properties of metal porous foam for conical shells consisting of two intriguing elastically restrained boundaries. Hung et al. [12] investigated the effect of the porous FG variable thickness for the toroidal shell on the nonlinear stability (buckling and post-buckling) under compressive loads and surrounded by the elastic foundation. Vinh and Huy [28] presented an inclusive analysis of the buckling, static bending and free vibration of the FG plates for sandwiches, including porosity distribution according to the finite element method with new hyperbolic shear deformation theory. Amir and Talha [29] employing finite element and high-order shear deformation technique, this research looked at the vibration of nonlinear thermo-elastic characteristics of FG porous double curve shallow shells. Keleshteri and Jelovica [30] employed high-order bidirectional porosity distributions to examine the free and forced vibration characteristics of FG porous beams. Nevertheless, there have only been a few studies on the FGM free vibration systems with porous metal formation. This investigation's objective is to carry out a study on the nonlinear analysis of free vibration of a simply-supported two-phase FGM cylindrical shell panel with porous as part of its research. In the present work, suppose that the FGM is constructed from ceramic and metal, mechanical characteristics are varied with reason disparate porosity distributions based on power-law distributions, with changes in the thickness direction. A novel model for the first-order shear deformation theory is formed to discover the nonlinear free vibration characteristics according to different FGM parameters. Utilizing the FEA strategy that is exemplified by ANSYS software, the results of mode and natural frequency forms of the FGM cylindrical shell with porous are provided here. The numerical findings for FG porous materials that are offered here are not found anywhere else in the literature, and as a consequence, should be of relevance to industrial applications. This study is organized into four parts. In the first section, theory of first-order shear deformation criteria is introduced, in addition to constitutive equations, features of FG porous structures, and an analytical vibration analysis of the porous cylindrical panel. The second section introduces numerical analysis and finite element simulation. Results and discussion are included in the third section. The last part includes study summaries and findings.

2 Models of Porous FGM Cylindrical Shell Panel

Consider a thick FGM cylindrical shell panel made of metal and ceramic, in which the lower surface is ceramic-rich and the upper surface is metal-rich, respectively. The FGM cylindrical panel is considered to carry porosities that distribute evenly and unevenly through the shell thickness direction (Fig. 1). The shell's thickness, Radius, and edges are represented by h, R, a, and b, respectively. To describe the shell's motion, a cartesian

coordinate system (x, y, z) on the center surface of the shell is employed, where z identifies the out-of-plane coordinate, and x and y determine the shell's in-plane coordinates.

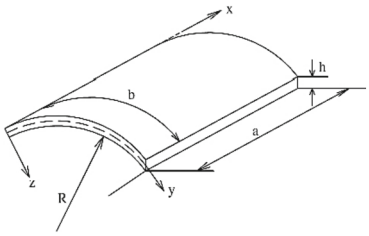

Fig. 1. The geometry of the cylindrical panel found on the FGM.

In addition, the power law, the sigmoid law, or the exponential law may be used to adequately represent the volume fraction of the FG cylindrical shell layers. Equation 1 makes the assumption that the distribution of the ceramic volume fraction Vc is governed by a power law [31]:

$$V_m + V_c = 1V_c = V_c(z) = \left(\frac{2z+h}{2h}\right)^g \tag{1}$$

where, Vc and Vm are volume fractions of ceramic and metal, respectively. g is the power-law index. When the value of g is equal to infinity, it indicates a fully metallic shell, whereas when the value of g is equal to zero, it denotes a fully ceramic shell. The fundamental mechanical properties of the FGM cylindrical shell panels, with a porosity volume ratio of G (G < 1), adopt the modified form of Eq. 2, assuming that porosities disperse equally in the ceramic and metal phases

$$P(z) = P_m + (P_c - P_m)\left(\frac{2z+h}{2h}\right)^g - \frac{G}{2}(P_c - P_m) \tag{2}$$

Pm and Pc represented the values of the material properties of the metal and ceramic components of the FG shells, respectively. Young's modulus (E) and mass density (ρ) are taken to change in the thickness direction for our current formulations, while Poisson's ratio (v) will be assumed to remain constant for simplicity based on earlier research.

2.1 Fundamental Equations

This study takes into account thick porous FGM cylindrical shell panels subjected to external loading with varying boundary conditions. As a result, the system of governing equations is established, and the nonlinear vibration of the cylindrical shell is determined using first-order shear deformation plate theory [32]:

$$\begin{aligned}
\tilde{u}(x, y, z, t) &= u(x, y, t) + z\phi_x(x, y, t), \\
\tilde{v}(x, y, z, t) &= v(x, y, t) + z\phi_y(x, y, t), \\
\tilde{w}(x, y, z, t) &= w(x, y, t)
\end{aligned} \tag{3}$$

where, (ϕ_x, ϕ_y) describes the transverse normal slopes about x- and y-axes at $(z = 0)$. The following equations serve as the basis for the strain-displacement relationships of the cylindrical shell:

$$\begin{Bmatrix} \varepsilon_x \\ \varepsilon_y \\ \gamma_{xy} \end{Bmatrix} = \begin{Bmatrix} \varepsilon_x^\circ \\ \varepsilon_y^\circ \\ \gamma_{xy}^\circ \end{Bmatrix} + z \begin{Bmatrix} \lambda_x \\ \lambda_y \\ \lambda_{xy} \end{Bmatrix}, \begin{Bmatrix} \gamma_{xz} \\ \gamma_{yz} \end{Bmatrix} = \begin{Bmatrix} \frac{\partial w}{\partial x} + \phi_x \\ \frac{\partial w}{\partial y} + \phi_y \end{Bmatrix} \tag{4}$$

$$\begin{Bmatrix} \varepsilon_x^\circ \\ \varepsilon_y^\circ \\ \gamma_{xy}^\circ \end{Bmatrix} = \begin{Bmatrix} \frac{\partial u}{\partial x} + \frac{1}{2}\left(\frac{\partial w}{\partial x}\right)^2 \\ \frac{\partial v}{\partial y} + \frac{1}{2}\left(\frac{\partial w}{\partial x}\right)^2 \\ \frac{\partial u}{\partial y} + \frac{\partial v}{\partial x} + \frac{\partial w}{\partial x}\frac{\partial w}{\partial y} \end{Bmatrix} \text{ and } \begin{Bmatrix} \lambda_x \\ \lambda_y \\ \lambda_{xy} \end{Bmatrix} = \begin{Bmatrix} \frac{\partial \phi_x}{\partial x} \\ \frac{\partial \phi_y}{\partial y} \\ \frac{\partial \phi_x}{\partial y} + \frac{\partial \phi_y}{\partial x} \end{Bmatrix}$$

In the planes (xz, yz), the x designates the transverse shear strain components $(\gamma_{xz}, \gamma_{yz})$. The nonlinear stress-strain constitutive relations at a general point inside the skin of the cylindrical shell can be expressed as:

$$\begin{Bmatrix} \sigma_x^{sh} \\ \sigma_y^{sh} \\ \tau_{xy}^{sh} \\ \tau_{xz}^{sh} \\ \tau_{yz}^{sh} \end{Bmatrix} = \begin{bmatrix} C_{11} & C_{12} & 0 & 0 & 0 \\ C_{12} & C_{22} & 0 & 0 & 0 \\ 0 & 0 & C_{44} & 0 & 0 \\ 0 & 0 & 0 & C_{55} & 0 \\ 0 & 0 & 0 & 0 & C_{66} \end{bmatrix} \begin{Bmatrix} \varepsilon_x \\ \varepsilon_y \\ \gamma_{xy} \\ \gamma_{xz} \\ \gamma_{yz} \end{Bmatrix} \tag{5}$$

For, $C_{11} = C_{22} = \frac{E(z)}{1-\nu^2}$, $C_{12} = \frac{\nu E(z)}{1-\nu^2}$, $C_{55} = C_{66} = \frac{E(z)}{2(1+\nu)}$.

Numerous studies have found the shear correction factor for homogeneous structures. Furthermore, some researchers have given a thickness-shear vibration value of $\frac{\pi^2}{12}$, but this will result in a different value for the FGM structure due to the material properties continuously changing in the thickness direction. So, the shear correction factor is denoted by (K_s), and its value is offered $\left(K = \frac{5}{6}\right)$ as [33]. The stress and moment resultants of the FGM porous cylindrical shell panel can be represented as,

$$\begin{aligned} &N_x = \int_{-\frac{h}{2}}^{\frac{h}{2}} \sigma_x^{sh} dz, N_y = \int_{-\frac{h}{2}}^{\frac{h}{2}} \sigma_y^{sh} dz, N_{xy} = \int_{-\frac{h}{2}}^{\frac{h}{2}} \tau_{xy}^{sh} dz, (Q_x, Q_y) = \int_{-\frac{h}{2}}^{\frac{h}{2}} K_s\left(\tau_{xz}^{sh}, \tau_{yz}^{sh}\right) dz, M_x = \int_{-\frac{h}{2}}^{\frac{h}{2}} \sigma_x^{sh} z dz, \\ &M_y = \int_{-\frac{h}{2}}^{\frac{h}{2}} \sigma_x^{sh} z dz, \ M_{xy} = \int_{-\frac{h}{2}}^{\frac{h}{2}} \tau_x^{sh} z dz \end{aligned} \tag{6}$$

where,

$$\begin{aligned} &N_x = I_{10}\varepsilon_x^\circ + I_{20}\varepsilon_y^\circ + I_{11}\frac{\partial \phi_x}{\partial x} + I_{21}\frac{\partial \phi_y}{\partial y}, \ N_y = I_{20}\varepsilon_x^\circ + I_{10}\varepsilon_y^\circ + I_{21}\frac{\partial \phi_x}{\partial x} + I_{11}\frac{\partial \phi_y}{\partial y} \\ &N_{xy} = I_{30}\gamma_{xy}^\circ + 2I_{31}\left(\frac{\partial \phi_x}{\partial y} + \frac{\partial \phi_y}{\partial x}\right), \ M_x = I_{11}\varepsilon_x^\circ + I_{21}\varepsilon_y^\circ + I_{12}\frac{\partial \phi_x}{\partial x} + I_{22}\frac{\partial \phi_y}{\partial y} \\ &M_y = I_{21}\varepsilon_x^\circ + I_{11}\varepsilon_y^\circ + I_{22}\frac{\partial \phi_x}{\partial x} + I_{12}\frac{\partial \phi_y}{\partial y}, \ M_{xy} = I_{31}\gamma_{xy}^\circ + I_{32}\left(\frac{\partial \phi_x}{\partial y} + \frac{\partial \phi_y}{\partial x}\right) \\ &Q_x = K_s I_{30}\gamma_{xz}, Q_y = K_s I_{30}\gamma_{yz}. \end{aligned} \tag{7}$$

The nonlinear governing motion equations of a porous FGM cylindrical shell panel are given below,

$$\begin{aligned}
\delta u &: \frac{\partial N_x}{\partial x} + \frac{\partial N_{xy}}{\partial y} = I_0 \frac{\partial^2 u}{\partial t^2} + I_1 \frac{\partial^2 \phi_x}{\partial t^2} \\
\delta v &: \frac{\partial N_{xy}}{\partial x} + \frac{\partial N_y}{\partial y} = I_0 \frac{\partial^2 v}{\partial t^2} + I_1 \frac{\partial^2 \phi_y}{\partial t^2} \\
\delta w &: \frac{\partial Q_x}{\partial x} + \frac{\partial Q_y}{\partial y} + N_x \frac{\partial^2 w}{\partial x^2} + 2N_{xy} \frac{\partial^2 w}{\partial x \partial y} \\
&+ N_y \frac{\partial^2 w}{\partial y^2} + q + \frac{N_y}{R} = I_0 \frac{\partial^2 w}{\partial t^2} \\
\delta \phi_x &: \frac{\partial M_x}{\partial x} + \frac{\partial M_{xy}}{\partial y} - Q_x = I_2 \frac{\partial^2 \phi_x}{\partial t^2} + I_1 \frac{\partial^2 u}{\partial t^2} \\
\delta \phi_y &: \frac{\partial M_{xy}}{\partial x} + \frac{\partial M_y}{\partial y} - Q_y = I_2 \frac{\partial^2 \phi_y}{\partial t^2} + I_1 \frac{\partial^2 v}{\partial t^2}
\end{aligned} \tag{8}$$

By submitting stress function f (x, y) as follow:

$$N_x = \frac{\partial^2 f}{\partial y^2}, \; N_y = \frac{\partial^2 f}{\partial x^2}, \; N_{xy} = -\frac{\partial^2 f}{\partial x \partial y} \tag{9}$$

Equation (9) is substituted into the first two equations of Eq. (8) to yield;

$$\frac{\partial^2 u}{\partial t^2} = -\frac{I_1}{I_0} \frac{\partial^2 \phi_x}{\partial t^2}, \quad \frac{\partial^2 v}{\partial t^2} = -\frac{I_1}{I_0} \frac{\partial^2 \phi_y}{\partial t^2} \tag{10}$$

Replacing (10) into the remaining three equations of Eq. (8), get,

$$\begin{aligned}
\delta w &: \frac{\partial Q_x}{\partial x} + \frac{\partial Q_y}{\partial y} + N_x \frac{\partial^2 w}{\partial x^2} + 2N_{xy} \frac{\partial^2 w}{\partial x \partial y} + N_y \frac{\partial^2 w}{\partial y^2} + q + \frac{N_y}{R} = I_0 \frac{\partial^2 w}{\partial t^2} \\
\delta \phi_x &: \frac{\partial M_x}{\partial x} + \frac{\partial M_{xy}}{\partial y} - Q_x = \left(I_2 - \frac{I_1^2}{I_0} \right) \frac{\partial^2 \phi_x}{\partial t^2} \\
\delta \phi_y &: \frac{\partial M_{xy}}{\partial x} + \frac{\partial M_y}{\partial y} - Q_y = \left(I_2 - \frac{I_1^2}{I_0} \right) \frac{\partial^2 \phi_y}{\partial t^2}
\end{aligned} \tag{11}$$

Through Eqs. (7) yield,

$$\begin{aligned}
\varepsilon_x^o &= A_{22} N_x - A_{12} N_y - B_{11} \frac{\partial \phi_x}{\partial x} - B_{12} \frac{\partial \phi_y}{\partial y} \\
\varepsilon_y^o &= A_{11} N_y - A_{12} N_x - B_{21} \frac{\partial \phi_x}{\partial x} - B_{22} \frac{\partial \phi_y}{\partial y} \\
\gamma_{xy}^o &= A_{66} N_{xy} - B_{66} \left(\frac{\partial \phi_x}{\partial y} + \frac{\partial \phi_y}{\partial x} \right)
\end{aligned} \tag{12}$$

The compatibility equation must be used to add an equation,

$$\frac{\partial^2 \varepsilon_x^{\circ}}{\partial y^2} + \frac{\partial^2 \varepsilon_y^{\circ}}{\partial x^2} - \frac{\partial^2 \gamma_{xy}^{\circ}}{\partial x \partial y} = \frac{\partial^2 w^2}{\partial x \partial y} - \frac{\partial^2 w}{\partial x^2}\frac{\partial^2 w}{\partial y^2} - \frac{1}{R}\frac{\partial^2 w}{\partial x^2} \tag{13}$$

Equation (12) is inserted into Eq. (7) and then into Eq. (11), which results in;

$$\begin{aligned} T_{11}(w) + T_{12}(\phi_x) + T_{13}\left(\phi_y\right) + S_1(w, f) + q &= I_0 \frac{\partial^2 w}{\partial t^2}, \\ T_{21}(w) + T_{22}(\phi_x) + T_{23}\left(\phi_y\right) + R_2(f) &= \left(I_2 - \frac{I_1^2}{I_0}\right)\frac{\partial^2 \phi_x}{\partial t^2}, \\ T_{31}(w) + T_{32}(\phi_x) + T_{33}\left(\phi_y\right) + R_3(f) &= \left(I_2 - \frac{I_1^2}{I_0}\right)\frac{\partial^2 \phi_y}{\partial t^2} \end{aligned} \tag{14}$$

When Eq. (12) is replaced with Eq. (13) and the stress functions, it provides the following formalization for the compatibility of FGM porous cylindrical shell panels

$$\left(\begin{array}{c} A_{11}\frac{\partial^4 f}{\partial x^4} + A_{22}\frac{\partial^4 f}{\partial y^4} + (A_{66} - 2A_{12})\frac{\partial^4 f}{\partial x^2 \partial y^2} - B_{21}\frac{\partial^3 \phi_x}{\partial x^3} - B_{12}\frac{\partial^3 \phi_y}{\partial y^3} + \\ (B_{66} - B_{11})\frac{\partial^3 \phi_x}{\partial x \partial y^2} + (B_{66} - B_{22})\frac{\partial^3 \phi_y}{\partial x^2 \partial y} - \left(\frac{\partial^2 w^2}{\partial x \partial y} - \frac{\partial^2 w}{\partial x^2}\frac{\partial^2 w}{\partial y^2} - \frac{1}{R}\frac{\partial^2 w}{\partial x^2}\right) \end{array}\right) = 0 \tag{15}$$

2.2 Nonlinear Vibration Analysis

In this paper, suppose that the porous FGM shell is subjected to impact of the uniformly distributed transverse load $q = Q \sin \Omega t$ with four edges simply supported boundary conditions:

$$\begin{aligned} w = N_{xy} = \phi_y = 0, \ \text{at} \ \ x = 0, \ a \\ w = N_{xy} = \phi_x = 0, \ \text{at} \ \ y = 0, \ b \end{aligned} \tag{16}$$

The next equations are desired to apply to the displacements in the present cases that satisfy the assumed boundary conditions [34]:

$$\begin{aligned} w(x, y, t) &= W(t) \sin \lambda_m x \ \sin \delta_n y \\ \phi_x(x, y, t) &= \Phi_x(t) \cos \lambda_m x \ \sin \delta_n y \\ \phi_y(x, y, t) &= \Phi_y(t) \sin \lambda_m x \ \cos \delta_n y \end{aligned} \tag{17}$$

Replacing (17) with (15), gain;

$$f(x, y, t) = \tilde{A}_1(t) \cos 2\lambda_m x + \tilde{A}_2(t) \cos 2\delta_n y + \tilde{A}_3(t) \sin \lambda_m x \ \sin \ \delta_n y$$

$$\tilde{A}_1(t) = \frac{\delta_n^2}{32 A_{11} \lambda_m^2} W^2; \ \tilde{A}_2(t) = \frac{\lambda_m^2}{32 A_{22} \delta_n^2} W^2$$

$$\tilde{A}_3(t) = \frac{\left(\frac{W}{R}\right) + \left(B_{21}\lambda_m^3 + (B_{11} - B_{66})\lambda_m \delta_n^2\right)\Phi_x(t) + \left(\delta_n^3 B_{12} + (B_{22} - B_{66})\lambda_m^2 \delta_n\right)\Phi_y(t)}{\left(A_{11}\lambda_m^4 + A_{22}\delta_n^4 + (A_{66} - 2A_{12})\lambda_m^2 \delta_n^2\right)} \tag{18}$$

After minor adjustments, the system of nonlinear motion equations in terms of displacements is derived by introducing the formula (17 and 18) into (14) and using the Galerkin method;

$$t_{11}W + t_{12}\Phi_x + t_{13}\Phi_y + t_{14}W\Phi_x + t_{15}W\Phi_y + t_{16}W + t_{17}W^2 + t_{18}W^3 + L_{32}q = I_0\frac{d^2W}{dt^2}$$

$$\begin{aligned} t_{21}W + t_{22}\Phi_x + t_{23}\Phi_y + n_7W + n_2W^2 &= \tilde{\rho}_1\ddot{\Phi}_x, \\ t_{31}W + t_{32}\Phi_x + t_{33}\Phi_y + n_9W + n_4W^2 &= \tilde{\rho}_1\ddot{\Phi}_y, \end{aligned} \tag{19}$$

The natural frequencies of the FGM porous cylindrical shell are obtained by solving Eq. (20), setting $q = 0$, and taking the linear components of Eq. (19):

$$\begin{vmatrix} t_{11} + t_{16} + I_0\omega^2 & t_{12} & t_{13} \\ t_{21} + n_1 & t_{22} + \widetilde{\rho}_1\omega^2 & t_{23} \\ t_{31} + n_3 & t_{32} & t_{33} + \widetilde{\rho}_1\omega^2 \end{vmatrix} = 0 \tag{20}$$

Three answers to Eq. (20) correspond to the axial, circumferential, and radial angular frequencies of the porosity FGM cylindrical shells. One with the lowest frequency is taken into account. The porosity FGM cylindrical shells panel subjected to orderly distributed load $q = Qsin\Omega t$ is considered, Eq. (19) becomes:

$$I_0\frac{d^2W}{dt^2} - t_{11}W - t_{12}\Phi_x - t_{13}\Phi_y - t_{14}W\Phi_x - t_{15}W\Phi_y - t_{16}W - t_{17}W^2 - t_{18}W^3 = L_{32}Q\sin\Omega t$$

$$\begin{aligned} t_{21}W + t_{22}\Phi_x + t_{23}\Phi_y + n_1W + n_2W^2 &= \tilde{\rho}_1\ddot{\Phi}_x \\ t_{31}W + t_{32}\Phi_x + t_{33}\Phi_y + n_3W + n_4W^2 &= \tilde{\rho}_1\ddot{\Phi}_y \end{aligned} \tag{21}$$

The nonlinear dynamic responses of a porous FGM cylindrical shell panel can be calculated using the fourth-order Runge-Kutta technique by solving Eq. (21) with the following initial conditions: $W(0) = 0$. When the second and third equations relating to (Φ_x, Φ_y), are solved from Eq. (21), the results are then substituted into the first equation to yield:

$$I_0\frac{d^2W}{dt^2} - (a_1 + a_2)W - (a_3 + a_4 + a_6 + r_{17})W^2 - (a_5 + r_{18})W^3 = L_{32}Q\sin\Omega t \tag{22}$$

The fundamental natural frequencies of the cylindrical shell may be calculated as follows:

$$\omega_{mn} = \sqrt{\frac{-(a_1 + a_2)}{I_0}} \tag{23}$$

3 Numerical Investigation

Using numerical methodologies is one way in which one may validate the precision of the analytical method that has been suggested. Problems may be solved using a wide variety of numerical methodologies, although the method of finite elements (FEM) [35] is considered to be the most accurate. The finite element method (FEM) that is outlined by the ANSYS software (Version 2020 R1) was used in this investigation. The construction of a three-dimensional prototype of the Functionally graded cylindrical shell panel, as shown in Fig. 2, is followed by the application of the matching shell's sides boundary conditions, which are subjected to modal study. In addition, as can be seen in Fig. 3, the prototype has been meshed with an 8-nodes SOLID186 slices type, which has resulted in a total of 19360 slices and 137922 nodes. This element type is a significant basic element that is used in the representation of structural models. As shown in Fig. 4 [36], the component consists of a higher-order solid element having 20 nodes that has quadratic spatial characteristics and three freedom degrees for translations along the normal axes. The equation that is used to determine the mechanical characteristics of the FGMs layers as follows: (2). The modal analysis for the selected models is carried out to determine the free vibration characteristics both natural frequencies and mode shapes, as shown in Fig. 5. This is done on the basis of the various factors that were described before.

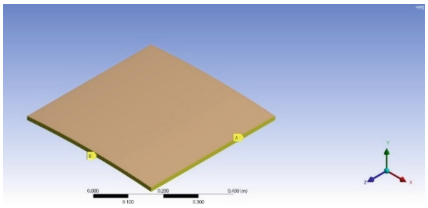

Fig. 2. FGM cylindrical shell panel

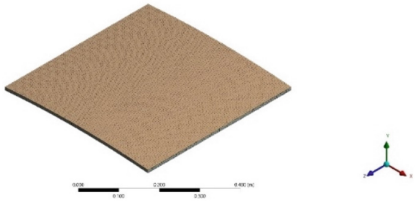

Fig. 3. Meshed Model

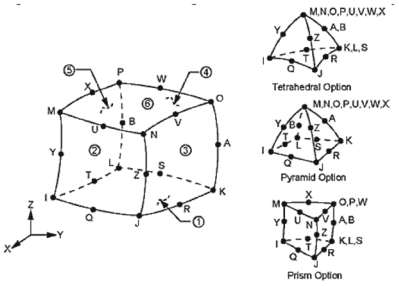

Fig. 4. Structural geometry of element type SOLID 186

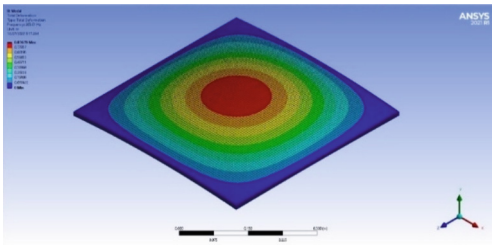

Fig. 5. View of the modular analysis of the FGM cylindrical shell

4 Results and Discussion

In this study, a novel mathematical form was developed to analyze the natural frequencies and modes of vibration of FGM cylindrical shell panels supported by just a simply support with uniform porosity distribution based on power-law distribution. Influences of different properties on frequency parameters are analyzed. The material properties of numerous individual materials that were used in this investigation are presented in Table 1. The analytical solution was also verified using the (ANSYS 2020 R1) software that is available for purchase, and the results were tabulated and presented using a variety of curves. Assume that the dimensions of the cylindrical shell are R = 3 m, a = b = 0.5 m., porosity factor (0.1, 0.2, and 0.3), the power-law distribution g = 2, and FG thickness (h = 10, 14, and 16 mm).

Table 1. The material properties of many individual materials

Material Property	FG core	
	Aluminum (Al)	Ceramic (Al2O3)
Modulus of Elasticity, GPa	70	380
Mass density, Kg/m^3	2702	3800
Poisson's ratio	0.3	0.3

Table 2 demonstrates both analytical and numerical findings for the cylindrical panel's natural frequencies for a variety of porosity factors. According to the information shown in Table 2, the thickness of the FG has a considerable impact on the frequency characteristics. Good agreements are reached between analytical analysis tests and numerical tests when the percentage of difference between the two is less than 0.9%. When the porosity factor goes up, the natural frequencies go down because the material stiffness of the goes down. On the other hand, when the panel FG thickness goes up, the natural frequency goes up because the panels get better as the Functionally graded core thickness goes up. This can be seen as a consequence of the findings in Table 2, which show that the natural frequencies go down when the porosity factor goes up. Accordingly, the first six deflections of three-dimensional mode shapes are shown for FGM in Fig. 6 when the material is simply supported in the form of porous cylindrical shell panels with the following parameters: a gradient index of (g = 0.5), a porosity ratio of (g = 30%), a = b = 0.5 m, R = 3, m = n = 1, and a thickness of 10 mm for the FGM. In a like way, it's also possible to depict other 3D mode shapes that are supported by a variety of edge conditions.

Figures 7 and 8 illustrate, respectively, the impacts of the material gradient factor (g) on the dynamic response and natural frequency of cylindrical panels with three different porosity values. These panels were designed to test the effectiveness of the material gradient parameter. Due to a reduction in the material's rigidity, shown that the natural frequency decline whenever the gradient indicator (g) increases, and the dynamic of nonlinear response expands in three porosity magnitudes of (10, 20, and

30%). Additionally, according to Eq. 2, the amount of metal increases while a volume of ceramic decreases, which results in a decrease in shell stiffness. The influence that the porosity factor, denoted by the symbol G, has on the dynamic of nonlinear response is seen in Fig. 9. There are three different levels of porosity that are taken into consideration: G = 10%, G = 20%, and G = 30%. As can be seen, increasing the pores results in a greater amplitude deflection of FGM cylindrical shells. This is something that can be noticed.

Analytical findings of the dynamic nonlinear response of the cylindrical shells with varying FG core thicknesses are shown in Fig. 10. (10, 15, and 20 mm). Figure 9 illustrates that the intensity of the dynamic of nonlinear response diminishes as the Functionally graded thickness of the shells grows. This is due to the fact that the stiffness of the FG panel increases as the Functionally graded thickness does.

Table 2. The FGM cylindrical panels' natural frequency with a power law index of g = 2.

Thickness	Porosity %	Analytical	Numerical	Discrepancy %
10	0.1	317.8349	315.35	0.63
	0.2	298.4475	296.66	0.67
	0.3	265.8474	265.61	0.075
14	0.1	400.8333	397.38	0.75
	0.2	372.2816	369.95	0.8
	0.3	322.9525	323.17	0.3
16	0.1	444.8098	440.7	0.9
	0.2	411.6792	408.92	0.72
	0.3	353.9510	354.32	0.28

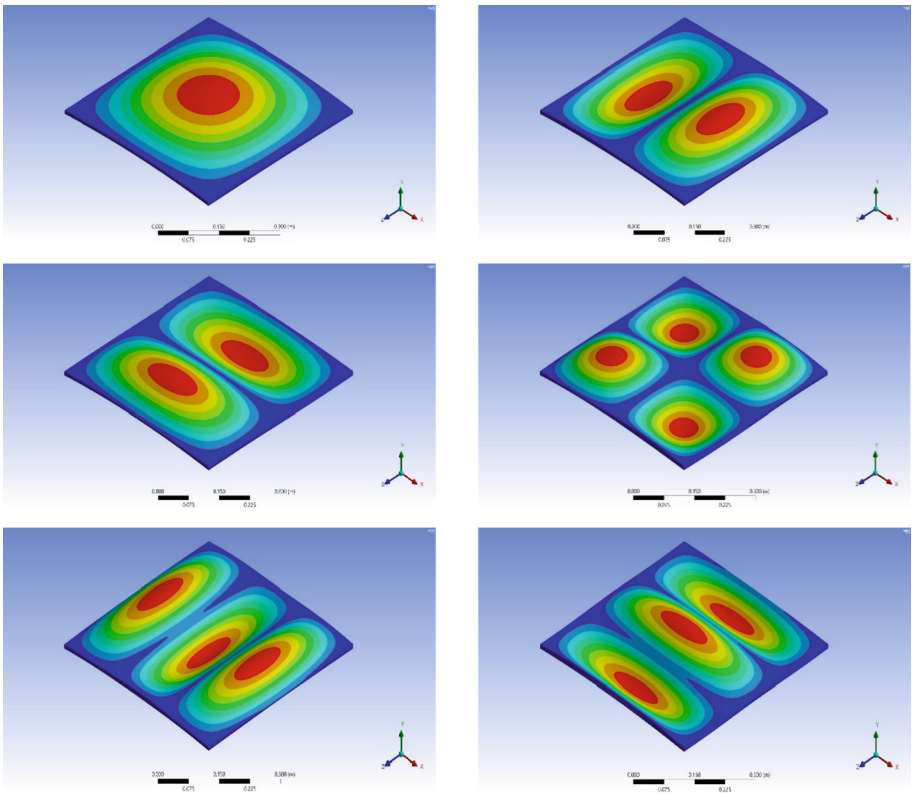

Fig. 6. The initial six mode shapes of Porous FGM simply supported cylindrical panels at G = 0.3, g = 2.

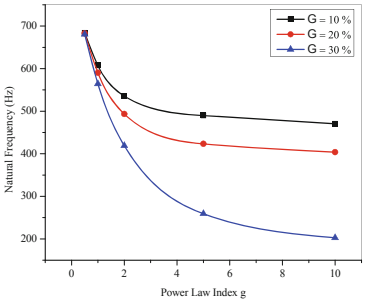

Fig. 7. The result of applying the power law index on porous FGM cylindrical panel was the following natural frequency results

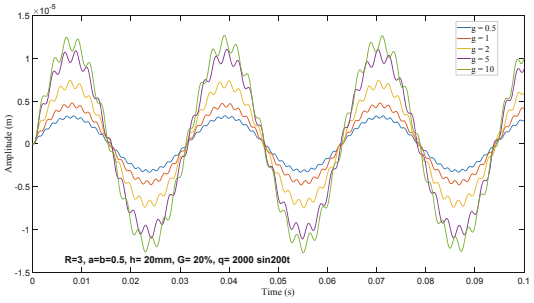

Fig. 8. A look at how the gradient index of a material affects the dynamic response of porous cylindrical shells made from fibrous graphene (FGM).

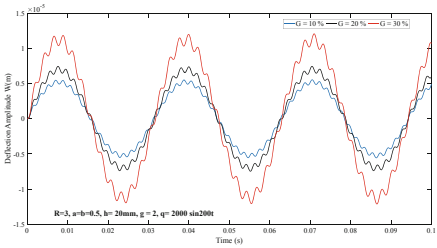

Fig. 9. The influence of porosity on the dynamic response of cylindrical panels

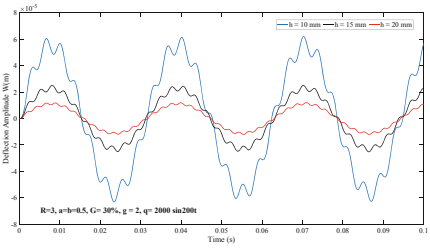

Fig. 10. Cylindrical shells made with porous FGM vibrate with varying FGM thicknesses.

5 Conclusion

In the current work, the nonlinear free vibration characteristics of an FG two-phase porous cylindrical shell with a simply supported boundary condition based on the FSDT are developed. A simply supported cylindrical shell's analytical formulation is presented in order to calculate the nonlinear free dynamic behavior. In order to validate the findings of an analytical solution, a numerical analysis was carried out with the assistance of ANSYS 2021 R1. Also, on deflection-time curve and natural frequency, the research findings for material gradient, porous parameter, and FG thickness are displayed. Based on the findings, it can be deduced that the porosity parameter does, in fact, have some kind of influence on the essential natural frequency of the FG cylindrical panels. According to the findings, the natural frequencies go up when the porosity parameter goes down, but they go down when the stiffness of the material goes up. This is because the natural frequencies are more sensitive to changes in the rigidity of the material. In addition, a downward shift in the amplitude-time curve was seen whenever the porosity factor was raised.

Appendix

$$I_{10} = \frac{E_1}{1-\upsilon^2}, I_{20} = \frac{\upsilon E_1}{1-\upsilon^2}, I_{30} = \frac{E_1}{2(1+\upsilon)}, I_{11} = \frac{E_2}{1-\upsilon^2}, I_{21} = \frac{\upsilon E_2}{1-\upsilon^2}, I_{31} = \frac{E_2}{2(1+\upsilon)},$$

$$I_{12} = \frac{E_3}{1-\upsilon^2}, I_{22} = \frac{\upsilon E_3}{1-\upsilon^2}, I_{32} = \frac{E_3}{2(1+\upsilon)},$$

$$A_{11} = \frac{1}{\Delta} I_{10}, A_{22} = \frac{1}{\Delta} I_{10}, A_{12} = \frac{I_{20}}{\Delta}, A_{66} = \frac{1}{I_{30}}, \Delta = I_{10}^2 - I_{20}^2, B_{11} = A_{22} I_{11} - A_{12} I_{21}, B_{22} = A_{11} I_{11} - A_{12} I_{21},$$

$$B_{12} = A_{22} I_{21} - A_{12} I_{11}, B_{21} = A_{11} I_{21} - A_{12} I_{11}, B_{66} = \frac{I_{31}}{I_{30}}, D_{11} = I_{12} - B_{11} B_{12} - I_{21} B_{21}, D_{22} = I_{22} - B_{22} I_{11} - I_{21} B_{12},$$

$$D_{12} = I_{22} - B_{12}I_{11} - I_{21}B_{22}, D_{21} = I_{22} - B_{21}I_{11} - I_{21}B_{11}, D_{66} = I_{32} - I_{31}B_{66},$$

$$\mathrm{T}_{11}(w) = K_s I_{30}\frac{\partial^2 w}{\partial x^2} + K_s I_{30}\frac{\partial^2 w}{\partial y^2}, T_{12}(\phi_x) = K_s I_{30}\frac{\partial \phi_x}{\partial x},$$

$$\mathrm{T}_{13}(\phi_y) = K_s I_{30}\frac{\partial \phi_y}{\partial y}, R_1(w,f) = \frac{\partial^2 f}{\partial x^2}\frac{\partial^2 w}{\partial x^2} - 2\frac{\partial^2 f}{\partial x \partial y}\frac{\partial^2 w}{\partial x \partial y} + \frac{\partial^2 f}{\partial x^2}\frac{\partial^2 w}{\partial y^2} + \frac{1}{R}\frac{\partial^2 f}{\partial x^2},$$

$$\mathrm{T}_{21}(w) = -K_s I_{30}\frac{\partial w}{\partial x}, T_{22}(\phi_x) = D_{11}\frac{\partial^2 \phi_x}{\partial x^2} + D_{66}\frac{\partial^2 \phi_y}{\partial y^2} - K_s I_{30}\phi_x, \mathrm{T}_{23}(\phi_y) = (D_{12} + D_{66})\frac{\partial^2 \phi_y}{\partial x \partial y},$$

$$R_2(f) = B_{21}\frac{\partial^3 f}{\partial x^3} + (B_{11} - B_{66})\frac{\partial^3 f}{\partial x \partial y^2}, \mathrm{T}_{31}(w) = -K_s I_{30}\frac{\partial w}{\partial y}, \mathrm{T}_{32}(\phi_x) = (D_{21} + D_{66})\frac{\partial^2 \phi_x}{\partial x \partial y},$$

$$\mathrm{T}_{33}(\phi_y) = D_{22}\frac{\partial^2 \phi_y}{\partial y^2} + D_{66}\frac{\partial^2 \phi_y}{\partial x^2} - K_s I_{30}\phi_y, R_3(f) = B_{12}\frac{\partial^3 f}{\partial y^3} + (B_{22} - B_{66})\frac{\partial^3 f}{\partial x^2 \partial y},$$

References

1. Ninh, D.G., Ha, N.H., Long, N.T., Tan, N.C., Tien, N.D., Dao, D.V.: Thermal vibrations of complex-generatrix shells made of sandwich CNTRC sheets on both sides and open/closed cellular functionally graded porous core. Thin-Walled Struct. **182** (2023). https://doi.org/10.1016/j.tws.2022.110161
2. Yang, Z., et al.: Dynamic buckling of rotationally restrained FG porous arches reinforced with graphene nanoplatelets under a uniform step load. Thin-Walled Struct. **166** (2021). https://doi.org/10.1016/j.tws.2021.108103
3. Viet Hoang, V.N., Tien, N.D., Ninh, D.G., Thang, V.T., Truong, D.V.: Nonlinear dynamics of functionally graded graphene nanoplatelet reinforced polymer doubly-curved shallow shells resting on elastic foundation using a micromechanical model. J. Sandw. Struct. Mater. **23**(7), 3250–3279 (2021). https://doi.org/10.1177/1099636220926650
4. Njim, E., Bakhi, S., Al-Waily, M.: Experimental and numerical flexural properties of sandwich structure with functionally graded porous materials. Eng. Technol. J. **40**(1), 137–147 (2022). https://doi.org/10.30684/etj.v40i1.2184
5. Mouthanna, A., Bakhy, S.H., Al-Waily, M.: Frequency of non-linear dynamic response of a porous functionally graded cylindrical panels. J. Teknol. **84**(6), 59–68 (2022). https://doi.org/10.11113/jurnalteknologi.v84.18422
6. Mouthanna, A., Bakhy, S.H., Al-Waily, M.: Analytical investigation of nonlinear free vibration of porous eccentrically stiffened functionally graded sandwich cylindrical shell panels. Iran. J. Sci. Technol. Trans. Mech. Eng. (2022). https://doi.org/10.1007/s40997-022-00555-4
7. Bagheri, H., Eslami, M.R., Kiani, Y.: Geometrically nonlinear response of FGM joined conical–conical shells subjected to thermal shock. Thin-Walled Struct. **182** (2023). https://doi.org/10.1016/j.tws.2022.110171
8. Zhu, C.S., Fang, X.Q., Liu, J.X.: Relationship between nonlinear free vibration behavior and nonlinear forced vibration behavior of viscoelastic plates. Commun. Nonlinear Sci. Numer. Simul. **117** (2023). https://doi.org/10.1016/j.cnsns.2022.106926
9. Li, Y.S., Liu, B.L.: Thermal buckling and free vibration of viscoelastic functionally graded sandwich shells with tunable auxetic honeycomb core. Appl. Math. Model. **108**, 685–700 (2022). https://doi.org/10.1016/j.apm.2022.04.019
10. Singh, A., Naskar, S., Kumari, P., Mukhopadhyay, T.: Viscoelastic free vibration analysis of in-plane functionally graded orthotropic plates integrated with piezoelectric sensors: time-dependent 3D analytical solutions. Mech. Syst. Signal Process. **184** (2023). https://doi.org/10.1016/j.ymssp.2022.109636

11. Sahu, N.K., Biswal, D.K., Joseph, S.V., Mohanty, S.C.: Vibration and damping analysis of doubly curved viscoelastic-FGM sandwich shell structures using FOSDT. Structures **26**, 24–38 (2020). https://doi.org/10.1016/j.istruc.2020.04.007
12. Hung, D.X., Tu, T.M., Van Long, N., Anh, P.H.: Nonlinear buckling and postbuckling of FG porous variable thickness toroidal shell segments surrounded by elastic foundation subjected to compressive loads. Aerosp. Sci. Technol. **107** (2020). https://doi.org/10.1016/j.ast.2020.106253
13. Ninh, D.G., Bich, D.H.: Nonlinear buckling of eccentrically stiffened functionally graded toroidal shell segments under torsional load surrounded by elastic foundation in thermal environment. Mech. Res. Commun. **72**, 1–15 (2016). https://doi.org/10.1016/j.mechrescom.2015.12.002
14. Ghobadi, A., Tadi Beni, Y., Kamil Żur, K.: Porosity distribution effect on stress, electric field and nonlinear vibration of functionally graded nanostructures with direct and inverse flexoelectric phenomenon. Compos. Struct. **259** (2021). https://doi.org/10.1016/j.compstruct.2020.113220
15. Esayas, L.S., Kattimani, S.: Effect of porosity on active damping of geometrically nonlinear vibrations of a functionally graded magneto-electro-elastic plate. Def. Technol. **18**(6), 891–906 (2022). https://doi.org/10.1016/j.dt.2021.04.016
16. Soleimani-Javid, Z., Arshid, E., Amir, S., Bodaghi, M.: On the higher-order thermal vibrations of FG saturated porous cylindrical micro-shells integrated with nanocomposite skins in viscoelastic medium. Def. Technol. **18**(8), 1416–1434 (2022). https://doi.org/10.1016/j.dt.2021.07.007
17. Keleshteri, M.M., Jelovica, J.: Analytical solution for vibration and buckling of cylindrical sandwich panels with improved FG metal foam core. Eng. Struct. **266** (2022). https://doi.org/10.1016/j.engstruct.2022.114580
18. HS, N.K., Kattimani, S., Nguyen-Thoi, T.: Influence of porosity distribution on nonlinear free vibration and transient responses of porous functionally graded skew plates. Def. Technol. **17**(6), 1918–1935 (2021). https://doi.org/10.1016/j.dt.2021.02.003
19. Srikarun, B., Songsuwan, W., Wattanasakulpong, N.: Linear and nonlinear static bending of sandwich beams with functionally graded porous core under different distributed loads. Compos. Struct. **276** (2021). https://doi.org/10.1016/j.compstruct.2021.114538
20. Chan, D.Q., van Thanh, N., Khoa, N.D., Duc, N.D.: Nonlinear dynamic analysis of piezoelectric functionally graded porous truncated conical panel in thermal environments. Thin-Walled Struct. **154** (2020). https://doi.org/10.1016/j.tws.2020.106837
21. Moradi-Dastjerdi, R., Behdinan, K.: Free vibration response of smart sandwich plates with porous CNT-reinforced and piezoelectric layers. Appl. Math. Model. **96**, 66–79 (2021). https://doi.org/10.1016/j.apm.2021.03.013
22. Yadav, A., Amabili, M., Panda, S.K., Dey, T.: Nonlinear analysis of cylindrical sandwich shells with porous core and CNT reinforced face-sheets by higher-order thickness and shear deformation theory. Eur. J. Mech. A/Solids **90** (2021). https://doi.org/10.1016/j.euromechsol.2021.104366
23. Binh, C.T., Van Long, N., Tu, T.M., Minh, P.Q.: Nonlinear vibration of functionally graded porous variable thickness toroidal shell segments surrounded by elastic medium including the thermal effect. Compos. Struct. **255** (2021). https://doi.org/10.1016/j.compstruct.2020.112891
24. Yaghoobi, H., Taheri, F.: Analytical solution and statistical analysis of buckling capacity of sandwich plates with uniform and non-uniform porous core reinforced with graphene nanoplatelets. Compos. Struct. **252** (2020). https://doi.org/10.1016/j.compstruct.2020.112700

25. Heshmati, M., Jalali, S.K.: Effect of radially graded porosity on the free vibration behavior of circular and annular sandwich plates. Eur. J. Mech. A/Solids **74**, 417–430 (2019). https://doi.org/10.1016/j.euromechsol.2018.12.009
26. Babaei, M., Hajmohammad, M.H., Asemi, K.: Natural frequency and dynamic analyses of functionally graded saturated porous annular sector plate and cylindrical panel based on 3D elasticity. Aerosp. Sci. Technol. **96** (2020). https://doi.org/10.1016/j.ast.2019.105524
27. Li, H., Hao, Y.X., Zhang, W., Liu, L.T., Yang, S.W., Wang, D.M.: Vibration analysis of porous metal foam truncated conical shells with general boundary conditions using GDQ. Compos. Struct. **269** (2021). https://doi.org/10.1016/j.compstruct.2021.114036
28. van Vinh, P., Huy, L.Q.: Finite element analysis of functionally graded sandwich plates with porosity via a new hyperbolic shear deformation theory. Def. Technol. **18**(3), 490–508 (2022). https://doi.org/10.1016/j.dt.2021.03.006
29. Amir, M., Talha, M.: Nonlinear vibration characteristics of shear deformable functionally graded curved panels with porosity including temperature effects. Int. J. Press. Vessel. Pip. **172**, 28–41 (2019)
30. Keleshteri, M.M., Jelovica, J.: Analytical assessment of nonlinear forced vibration of functionally graded porous higher order hinged beams. Compos. Struct. **298** (2022). https://doi.org/10.1016/j.compstruct.2022.115994
31. Liu, Y., Qin, Z., Chu, F.: Nonlinear forced vibrations of functionally graded piezoelectric cylindrical shells under electric-thermo-mechanical loads. Int. J. Mech. Sci. **201** (2021). https://doi.org/10.1016/j.ijmecsci.2021.106474
32. Quan, T.Q., Ha, D.T.T., Duc, N.D.: Analytical solutions for nonlinear vibration of porous functionally graded sandwich plate subjected to blast loading. Thin-Walled Struct. **170** (2022). https://doi.org/10.1016/j.tws.2021.108606
33. Zhou, K., Huang, X., Tian, J., Hua, H.: Vibration and flutter analysis of supersonic porous functionally graded material plates with temperature gradient and resting on elastic foundation. Compos. Struct. **204**, 63–79 (2018). https://doi.org/10.1016/j.compstruct.2018.07.057
34. Meksi, R., Benyoucef, S., Mahmoudi, A., Tounsi, A., Adda Bedia, E.A., Mahmoud, S.R.: An analytical solution for bending, buckling and vibration responses of FGM sandwich plates. J. Sandw. Struct. Mater. **21**(2), 727–757 (2019). https://doi.org/10.1177/1099636217698443
35. Rao, S.S.: The finite element method in engineering. Elsevier (2004)
36. Njim, E.K., Bakhy, S.H., Al-Waily, M.: Analytical and numerical investigation of buckling load of functionally graded materials with porous metal of sandwich plate. Mater Today Proc (2021). https://doi.org/10.1016/j.matpr.2021.03.557